

From Rule to Response: Neuronal Processes in the Premotor and Prefrontal Cortex

Jonathan D. Wallis and Earl K. Miller

Picower Center for Learning and Memory, RIKEN–MIT Neuroscience Research Center and Department of Brain and Cognitive Sciences, Massachusetts Institute of Technology, Cambridge, Massachusetts 02139

Submitted 30 January 2003; accepted in final form 4 May 2003

Wallis, Jonathan D., and Earl K. Miller. From rule to response: neuronal processes in the premotor and prefrontal cortex. *J Neurophysiol* 90: 1790–1806, 2003. First published May 7, 2003; 10.1152/jn.00086.2003. The ability to use abstract rules or principles allows behavior to generalize from specific circumstances (e.g., rules learned in a specific restaurant can subsequently be applied to any dining experience). Neurons in the prefrontal cortex (PFC) encode such rules. However, to guide behavior, rules must be linked to motor responses. We investigated the neuronal mechanisms underlying this process by recording from the PFC and the premotor cortex (PMC) of monkeys trained to use two abstract rules: “same” or “different.” The monkeys had to either hold or release a lever, depending on whether two successively presented pictures were the same or different, and depending on which rule was in effect. The abstract rules were represented in both regions, although they were more prevalent and were encoded earlier and more strongly in the PMC. There was a perceptual bias in the PFC, relative to the PMC, with more PFC neurons encoding the presented pictures. In contrast, neurons encoding the behavioral response were more prevalent in the PMC, and the selectivity was stronger and appeared earlier in the PMC than in the PFC.

INTRODUCTION

The ability to link sensory inputs to arbitrary actions is central to voluntary, goal-directed behavior. It depends on the integrity of the frontal lobe, a region whose many areas appear to be arranged in a processing hierarchy (Fuster 1997; Passingham 1993). The prefrontal cortex (PFC) is at the apex of this hierarchy and is thought to be responsible for implementing higher-order rules and strategies (Dias et al. 1996; Duncan 2001; Fuster 1997; Miller and Cohen 2001; Ragozzino et al. 1999; Ramus and Eichenbaum 2000; Roberts and Wallis 2000; Wise et al. 1996). It receives input from all sensory systems and sends projections to a variety of secondary motor areas, including the premotor cortex (PMC), which in turn project to more primary motor structures (Barbas and Pandya 1991; Pandya and Barnes 1987; Pandya and Yeterian 1990). Consistent with this hierarchy are observations that lesions of primary motor cortex, but not lesions of the PFC or PMC, impair the control of individual movements (Black 1975; Passingham et al. 1983). Instead, PFC or PMC damage disrupts performance of a classic test of volitional learning: conditional visuomotor tasks that require the learning of arbitrary associations between

sensory cues and limb movements (Bussey et al. 2001; Halsband and Passingham 1985; Murray et al. 2000; Parker and Gaffan 1998; Petrides 1985, 1982; Podbros et al. 1980; Stamm 1973). By contrast, such damage spares simpler, reflexive behaviors such as appetitive and orienting responses toward salient, rewarding objects (Grueninger and Pribram 1969; Stepien 1974).

Details about relative functional specializations or overlaps between the PFC and PMC remain largely unknown. Although neurophysiological studies have reported a greater incidence of sensory-related activity in the PFC and motor-related activity in the PMC (consistent with the PMC being functionally closer to motor output) there appears to be a great deal of overlap in these and other neuronal properties (Boussaoud and Wise 1993a,b; di Pellegrino and Wise 1991, 1993; Hernandez et al. 2002; Kalaska and Crammond 1995; Niki 1974b; Sakagami and Niki 1994a,b; Watanabe 1986a,b). For example, during conditional visuomotor tasks, neurons in both areas encode learned conditional visuomotor associations and show an evolution of activity that mirrors the acquisition of the associative rule (Asaad et al. 1998; Chen and Wise 1995a,b, 1996; Mitz et al. 1991). In general, however, little is known about similarities or differences between PFC and PMC neural mechanisms; they have rarely been compared under identical behavioral conditions.

Here, we compared and contrasted neural activity in the PFC and PMC by using a task that we had previously used to study PFC activity (Wallis et al. 2001a). It required monkeys to quickly switch between two rules, a type of behavior impaired after PFC damage in humans (Milner 1963; Nelson 1976; Owen et al. 1991; Stuss et al. 2000) and monkeys (Dias et al. 1996; Wallis et al. 2001b). In our task, an abstract rule (one not linked to a specific sensory input or motor output) intermediated between a stimulus and a response (Wallis et al. 2001a). The *same* rule required monkeys to release a lever if two successively presented (sample and test) pictures were identical, whereas the *different* rule required the lever release if the two pictures were different (Fig. 1). The experimental design thus permitted a full dissociation between the rules and the motor responses because, across trials, each motor response (hold and release) had to be made for each rule (*same* and *different*). This allowed us to disentangle their effects on neu-

Address for reprint requests: J. Wallis, E25-236, 45 Carleton Street, Massachusetts Institute of Technology, Cambridge, MA 02139 (E-mail: wallis@ai.mit.edu).

The costs of publication of this article were defrayed in part by the payment of page charges. The article must therefore be hereby marked “advertisement” in accordance with 18 U.S.C. Section 1734 solely to indicate this fact.

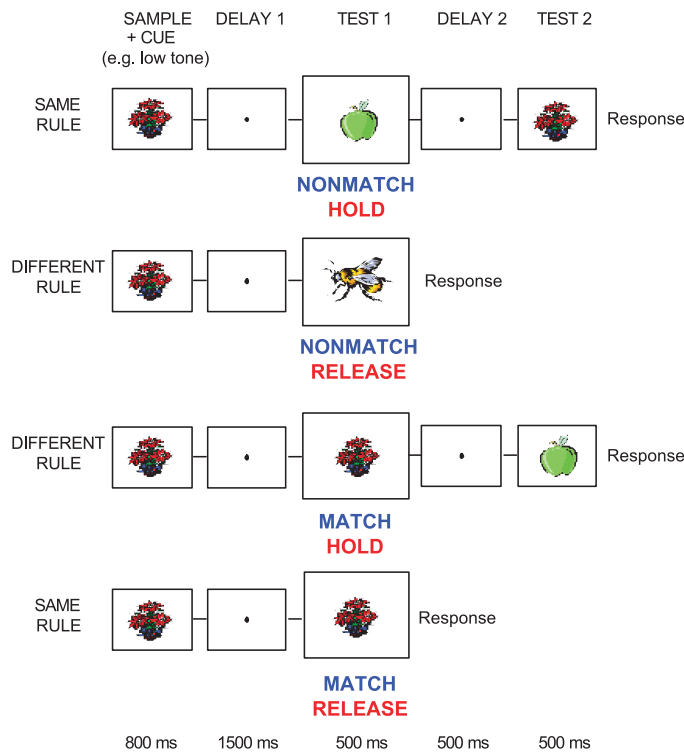


FIG. 1. Behavioral task. The monkey was presented with a sample picture, followed, after a short delay, by two successively presented test pictures. Depending on which of two rules was currently in effect (*same* or *different*) the monkey had to release a lever when the test picture either matched or did not match the sample picture. A cue stimulus, presented simultaneously with the sample picture, indicated to the monkey which rule was in effect on any given trial. See METHODS for further details.

ronal activity and explore their representations in the PFC and PMC. If the hierarchy described above is correct, then we would expect the PFC to be primarily involved in representing more high-level, abstract, rule-related information and PMC neurons to be more involved in generating motor commands. This would predict that rules would be more strongly encoded, and would tend to appear earlier, in the PFC than in the PMC. Here, we sought to test this hypothesis.

METHODS

Subjects and physiological procedures

The subjects were two adult rhesus monkeys (*Macaca mulatta*), one male and one female, weighing 5.0–6.0 kg. The monkeys were fitted with a head bolt for immobilization and a recording chamber was attached to the monkey’s skull. We recorded from the left PFC of monkey A and both the right and left PFC of monkey B. The positions of the recording chambers were determined using a 1.5-T magnetic resonance imaging (MRI) scanner. Monkeys were aligned in the scanner using a stereotactic frame and a positioning light beam. To record from a wide expanse of PFC, the chambers were repositioned several times. For the recordings from PMC we recorded bilaterally in both animals. The chambers were positioned to record from the dorsal PMC (primarily area F2), similar to previous studies that have compared neuronal properties in PFC and PMC (di Pellegrino and Wise 1991, 1993). The chambers were positioned with respect to the arcuate sulcus (Figs. 2 and 3), which is considered the defining boundary between PFC and PMC. Cortex anterior to this sulcus possesses a well-developed cell layer IV (Brodmann 1909; Petrides and Pandya 1994; Walker 1940) and receives projections from the

mediodorsal nucleus of the thalamus (Giguere and Goldman-Rakic 1988; Siwek and Pandya 1991), unlike the cortex posterior to this sulcus. There was a 5-mm separation in the anterior–posterior axis between the most posterior PFC recording and most anterior PMC recordings to ensure no accidental overlap. Indeed, the bulk of the recordings were separated by almost 10 mm.

Recordings were made using arrays of 8 tungsten dura-puncturing microelectrodes (FHC Instruments, Bowdoin, ME) and a grid (Crist Instruments, Damascus, MD) with 1-mm spacing. The approximate distance to lower the electrodes was determined from the MRI images and the electrodes were advanced using custom-built, manual micro-drives until they were located just above the cell layer. The electrodes were then slowly lowered into the cell layer until a neuronal wave-

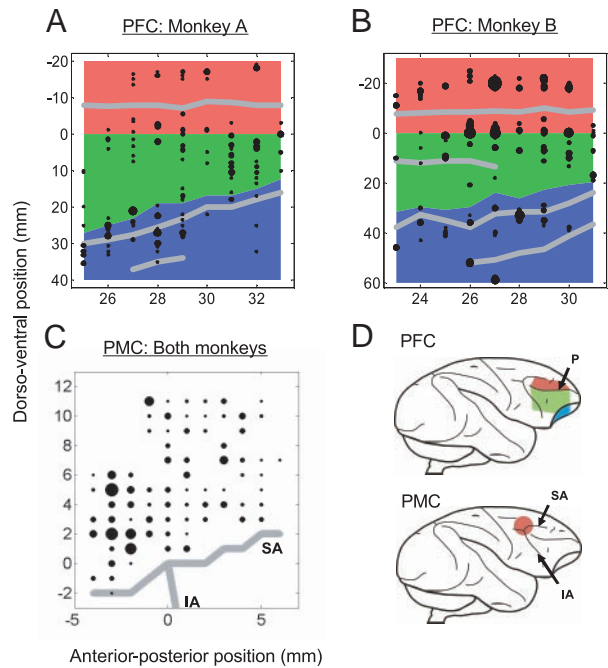


FIG. 2. A and B: flattened representation of prefrontal cortex (PFC) of both monkeys showing location of recording sites. Anterior–posterior position is measured from the interaural line, whereas dorsoventral position is measured from the ventral lip of the principal sulcus. The dorsolateral region (dorsal to the ventral lip of the principal sulcus) is shaded pink; ventrolateral region (from the ventral lip of the principal sulcus to the lateral lip of the lateral orbital sulcus) is shaded green; the orbitofrontal region (medial to the lateral lip of the lateral orbital sulcus) is shaded blue. In monkey A recording sites were located in the left hemisphere. In monkey B neurons were recorded from both hemispheres, but there was very little difference in the position of sulci between the two hemispheres (typically <10%). Thus we plotted sites on a single representation using the mean position of sulci. Size of dots is directly proportional to number of recordings performed at that location, ranging from one recording at smallest dots, to 11 recordings at largest. C: location of recording sites in premotor cortex (PMC). Anterior–posterior and dorsoventral positions are measured relative to the genu of the arcuate sulcus. There was no difference in position of sulci between the different monkeys and hemispheres relative to the genu (although the arcuate sulcus spur was not present in monkey A) and so all recording sites are plotted on a single diagram. Size of dots is directly proportional to number of recordings performed at that location, ranging from one recording at smallest dots, to 12 recordings at largest. D: diagrams showing location of PFC and PMC recording sites on lateral view of macaque brain. A single well was used to record from PMC (area 6/F2), indicated by the pink circle. Several wells were used to record from PFC, enabling neurons from the dorsolateral PFC (pink shading: areas 9, 46, and 9/46), ventrolateral PFC (green shading: areas 47/12 and 45), and orbitofrontal regions (blue shading: areas 11, 13, and 14) to be sampled. Area numbers refer to cytoarchitectonic scheme of Petrides and Pandya (1994). IA, inferior arcuate sulcus; SA, superior arcuate sulcus; P, principal sulcus; LO, lateral orbital sulcus; MO, medial orbital sulcus.

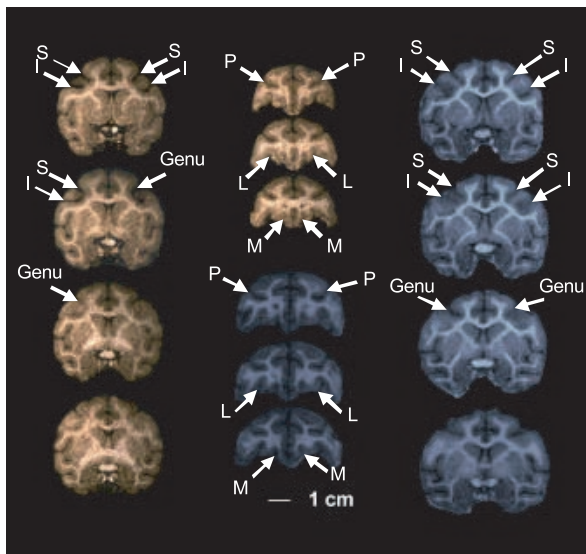


FIG. 3. Representative coronal MRI sections from the two monkeys, illustrating position of PFC and PMC sulci. *Left column*: four sections from monkey A, from AP +20 to AP +17, measured relative to interaural line. *Middle column*: three sections from monkey A (*top*) and three sections from monkey B (*bottom*) showing sections through PFC from AP +29 to AP +27. *Right column*: four sections from monkey B showing sections from AP +18 to AP +15. S, superior arcuate sulcus; I, inferior arcuate sulcus; Genu, genu of the arcuate sulcus (where the superior and inferior arcuate sulci meet); P, principal sulcus; L, lateral orbital sulcus; M, medial orbital sulcus.

form was obtained. We then waited 3 h for the brain to settle and thus ensure stability during the recording session, which typically lasted 2 h. Neurons were randomly sampled; no attempt was made to select neurons on the basis of responsiveness. To ensure that our recordings were of consistent quality, after each session we measured the impedance of the electrodes. Typically values were >1 megaohm ($M\Omega$). If values dropped below $0.5 M\Omega$ we would scrape the surface of the dura, or use dura-puncturing guide tubes constructed from 23-gauge hypodermic needles (Samuel Perkins, Quincy, MA) to enable electrodes to enter the brain with less loss of impedance.

Waveforms were digitized and analyzed off-line (Plexon Instruments, Dallas, TX). Approximately 20% of the channels were discarded, either because neuronal waveforms could not be clearly separated or because the waveforms did not remain stable throughout the entire session. Separation of neuronal waveforms was ensured by rejecting channels where more than 0.1% of the waveforms were separated by intervals of <2 ms. The modal number of electrodes (59%) had one discriminable waveform, 32% had two, and 8% had three. On average, slightly more neurons per electrode were obtained in the PMC (mean 1.6) compared with the PFC (mean 1.4, *t*-test, *d.f.* = 476, $P < 0.005$). PFC and PMC recordings were conducted sequentially.

Recording locations were reconstructed by measuring the position of the recording chambers using stereotaxic methods. These were then plotted onto the MRI sections (see above and Fig. 3) using commercial graphics software (CorelDraw, Ottawa, Canada). We confirmed the correspondence between the MRI sections and our recording chambers by mapping the position of the arcuate sulcus using neurophysiological recordings (i.e., a lack of signal indicating that the electrode was positioned in the sulcus). For the PFC recordings, the distance of each recording location along the cortical surface from the principal sulcus was then traced and measured. The positions of the other sulci, relative to the principal sulcus, were also measured in this way, allowing the construction of the unfolded cortical maps shown in Fig. 2.

All procedures were in accord with the National Institute of Health

guidelines and the recommendations of the MIT Animal Care and Use Committee.

Behavioral task

Trials began when the monkey grasped a lever and fixated a central fixation point (Fig. 1). Eye position was monitored throughout the session using an infrared monitoring system (ISCAN, Burlington, MA). Monkeys were required to keep their gaze within 1.5 deg of a central fixation point. If the monkey's gaze deviated outside of this window the trial was immediately terminated; breaks of fixation were not included in the overall error rates. Once the monkey had maintained central fixation for 800 ms, a sample picture was presented at the center of gaze for 800 ms, followed by a 1,500-ms delay, and then by a test picture (500 ms). For the *same* rule, the monkey released the lever if the test picture matched the sample. For the *different* rule they released the lever if the sample did not match; otherwise, they held the lever through a second delay (300 ms) until the appearance of another picture (500 ms) that always required a response. Thus only the test picture required a decision as to whether to hold or release the lever. The second delay and picture were used so that a behavioral response was required on each trial, ensuring that the monkeys were engaged in the task. The rule was signified with a brief (100-ms) cue coincident with sample onset (for monkey A, a drop of juice or a low tone indicated *same*, whereas no juice or a high tone indicated *different*; for monkey B, juice or a blue background indicated *same*, whereas no juice or a green background indicated *different*). A set of four pictures was used for each daily recording session. They were chosen at random from the internet, and reduced to 1.8° in size. The use of four pictures meant that the identity of the nonmatching test object could not be predicted and thus the monkeys needed to remember both the current sample picture and rule. Trials were randomized and balanced across all relevant features (cues, samples, rules, and responses). The monkeys completed about 700 correct trials per day at a consistent level of performance. They were very experienced with this task, having learned it over the course of several months and performed tens of thousands of trials after its acquisition.

Data analysis

The PFC neuron population is the same as from our previous report on the PFC alone (Wallis et al. 2001a). Here, we report on additional data collected from the PMC to compare and contrast neuronal activity between the areas. Only data from correct trials were used; there were insufficient incorrect trials to permit their analysis. Spike density histograms were constructed by averaging activity across the appropriate conditions, and then into 50-ms bins. There is nothing special about the order in which these two steps are performed because averaging into 50-ms bins and then across conditions is mathematically identical.

The time course of neuronal selectivity was examined by performing a sliding receiver operating characteristic (ROC) analysis. An ROC analysis measures the degree of overlap between two response distributions. For each selective neuron the preferred and unpreferred conditions were compared, giving two distributions, P and U respectively, of neuronal activity. For example, for a rule-selective neuron these distributions might be the neuron's firing rates when the *same* rule was in effect in comparison to the *different* rule. An ROC curve was then generated by taking each observed firing rate of the neuron and plotting the proportion of P that exceeded the value of that observation against the proportion of U that exceeded the value of that observation. The area under the ROC curve was then calculated. A value of 0.5 would indicate that the two distributions completely overlap (because for each value of the neuron's firing rate the proportion of P and U exceeding that value is equal), and thus the neuron is not selective. A value of 1.0, on the other hand, would indicate that the two distributions are completely separate (i.e., every value drawn

from U is exceeded by the entirety of P, whereas none of the values of P is exceeded by any of the values in U) and so the neuron is very selective. This method of analysis has the advantage that it is independent of the neuron's firing rate, and so can be used to compare neurons with different baseline firing rates and dynamic ranges. It is also nonparametric and so does not require the distributions to be Gaussian. Furthermore, the ROC value can be thought of as the probability that an independent observer could identify the condition that had been presented using the neuron's firing rate.

Starting from the baseline period of the trial, the ROC value was calculated for a 200-ms epoch. This was repeated in 10-ms increments until the entire trial had been analyzed. We used a relatively large time window (200 ms) that was incremented by small time steps (10 ms). This allowed good temporal resolution, but it caused neighboring time bins to be highly correlated with one another. However, our critical comparisons were always between different conditions (i.e., when activity related to the conditions began to diverge), rather than adjacent time bins, and so these correlations did not affect the analysis. From this analysis we were able to determine the latency at which selectivity appeared. It should be noted that smoothing the data using a sliding window means that the latency values should not be interpreted as exact values; we were interested purely in terms of comparing the relative latency of effects between the PFC and PMC. The criterion for selectivity was defined as the point at which the sliding ROC curve exceeded 0.6, for three consecutive 10-ms bins. This arbitrary criterion was chosen as one that, overall, yielded the best correspondence with latencies determined by examining spike histograms (e.g., compare Figs. 5 and 6). However, a wide range of criteria yielded essentially the same results (see following text). Latency values were computed for each neuron individually. Latency values across the population were typically not normally distributed, and so the median values were computed and comparisons between the populations used nonparametric statistics. A baseline period was defined as the 500 ms preceding the presentation of the sample picture (the last 500 ms of the fixation period) for neurons that showed selectivity during the sample and delay epoch, and the 500 ms preceding the presentation of the test picture (the last 500 ms of the delay epoch) for neurons that showed selectivity during the test epoch.

The differences we observed between the PFC and PMC were robust with respect to the precise criterion that we used to define the latency. We used a wide range of criteria: different ROC values (ranging from 0.55 to 1), a value of 3SDs greater than each neuron's ROC values during the baseline period, and a value that exceeded 99% of the neuron's baseline ROC values. Although these different criteria yielded different absolute latency values, the latency differences between the PFC and PMC that we report here were similar in all cases. We also ensured that the analysis was robust with respect to the precise time window that we used. Thus we examined all time windows from 75 to 500 ms in 25-ms increments (with windows smaller than 75 ms, we could not accumulate enough spikes to compute ROC values). All windows yielded the same pattern of significant differences between the PFC and the PMC.

We performed a power analysis to determine whether sufficient neurons had reached criterion to meaningfully compare the latency of selectivity between the two areas, particularly when concluding that there were no significant differences between populations. We estimated our minimum effect size as medium, corresponding to a "distance measure" of 0.5 (Cohen 1988). This is a measure of the difference between the mean of the sampling distribution if the null hypothesis was true and the mean of the sampling distribution if the null hypothesis was false, expressed in terms of the SD of the parent population. For comparison, the size of this "distance measure" for the difference in the latency of the rule selectivity between the PFC and PMC was 0.64. A power of 0.95 was desired, giving a required minimum sample size of 70 neurons. In comparison, for all statistical tests used in this study we evaluated Type I errors at 0.01, making a

Type II error five times as likely as a Type I error, a reflection of their estimated relative importance.

To further quantify the strength of encoding of the different aspects of the task, the trial was divided into three epochs, the 800 ms of the presentation of the sample picture, the 1,500 ms of the delay, and the 500 ms of the first test picture presentation. For each trial the total number of spikes that the neuron fired in each epoch was determined, and an ROC measure for the entire epoch was calculated. Because these values were not normally distributed, to compare the ROC values between the two areas we used a Wilcoxon's rank-sum test assessed at $P < 0.01$.

The ROC values were calculated for the entire population of neurons (which were not prescreened for selectivity or responsiveness; see METHODS). As a result, the ROC values were often close to 0.5. To ensure that the values were significantly different from chance we performed a bootstrap analysis. For each neuron, the trials were randomly assigned to the different behavioral conditions, and the ROC value calculated. This process was repeated 1,000 times for each neuron, and the mean ROC value was determined. A Wilcoxon's rank-sum test then compared these mean ROC values derived from the shuffled data to the actual ROC values.

We also compared the incidence of neurons encoding the different aspects of the task using an ANOVA. We defined rule-selective neurons as those that showed a significant difference in their firing rates between the two different rules, regardless of either the cue that was used to instruct the monkey, or the picture that was used as the sample stimulus. To consider the effect of all 3 factors on the neuron's firing rate it was necessary to use a 3-way ANOVA to analyze activity during the sample and delay epochs. The mean firing rate of the neuron in each epoch was compared, using the factors of the modality in which the cue was presented (monkey A: taste/auditory cue; monkey B: taste/visual cue), the rule that the cue signified (*same* or *different*), and which of the 4 pictures was presented as the sample stimulus. Thus a rule-selective neuron showed a main effect of rule, and no interaction with the other 2 factors. We also used this analysis to define picture-selective neurons (those that had a main effect of picture, and no interaction with the other 2 factors). Significance was assessed at $P < 0.01$. Differences in the prevalence of neurons between 2 areas (either PFC vs. PMC, or anterior PMC vs. posterior PMC) were assessed using a chi-square test at an alpha level of $P < 0.01$, whereas differences among 3 areas (a comparison between the dorsolateral PFC, ventrolateral PFC, and orbitofrontal cortex) were assessed using multiple chi-square tests with a Bonferroni-corrected alpha level of 0.0033.

During the test epoch 3 different processes were examined. First, neurons that encoded the test picture were identified using a Kruskal-Wallis one-way ANOVA on the firing rate of the neurons when the 4 different test pictures were presented. Second, neurons that encoded whether the test picture matched the sample picture were identified by performing a Wilcoxon's rank-sum test on the neuron's firing rate under both conditions. Finally, neurons that encoded the behavioral response were determined by performing a Wilcoxon's rank-sum test on the neuron's firing rate when the monkey had either to hold or to release the lever. In all cases significance was assessed at $P < 0.01$, and differences in the proportions of the neurons were determined using chi-square tests.

RESULTS

Behavior

Both monkeys were proficient at the task (monkey A 85% correct overall, and monkey B 93%; Table 1). Performance was significantly better during those sessions in which neurons were recorded from the PMC compared with the PFC (PFC: 93%, $n = 55$, PMC: 87%, $n = 17$; Wilcoxon's rank-sum test =

TABLE 1. Mean performance (percentage of trials that were correct) of the two monkeys, across the recording sessions from the two areas and across the different conditions

Rule		Monkey A		Monkey B	
Cue	Response	PFC	PMC	PFC	PMC
"Different" No juice	Release	90	91	96	97
	Hold	85	93	94	97
High tone/green background	Release	83	86	91	96
	Hold	78	91	86	94
"Same" Juice	Release	91	93	99	99
	Hold	89	93	94	98
Low tone/blue background	Release	80	86	89	92
	Hold	75	86	85	92

911, $P < 0.0005$). Performance on *same* and *different* trials was identical (*same*: 88%, *different*: 89%; Wilcoxon's matched-pairs signed-ranks test = 977, $n = 72$, $P > 0.1$). The monkeys had a bias toward holding rather than releasing the lever (hold: 90%, release: 87%; Wilcoxon's matched-pairs signed-ranks test = 277, $n = 72$, $P < 5 \times 10^{-8}$), and performed better for the juice/no juice cues than for the visual or auditory cues (juice/no juice: 93%, visual/auditory: 85%; Wilcoxon's matched-pairs signed-ranks test = 1, $n = 72$, $P < 1 \times 10^{-12}$).

The most consistent difference in reaction times was between the hold and release trials (Table 2). The monkeys released an average of 20 ms later to the first test picture (on release trials) compared with the second picture (on hold trials). This presumably reflects the fact that the first test picture requires a decision as to the correct behavioral response, unlike the second picture, which always requires a release. The reaction times on release trials, across the same and different rules, were virtually identical (median 374 and 373 ms, respectively), and there was also no difference in reaction times on release trials between the juice/no juice cues and the visual or auditory cues (median 373 and 374 ms, respectively). Monkey A tended to be faster on release trials during the sessions in which the PFC data were recorded (median 372 ms) compared with the PMC data (median 389 ms), whereas the opposite pattern was observed in monkey B (PFC: median 389 ms; PMC: median 357 ms).

For recording sessions, we used 4 novel pictures. This raised the possibility that the monkeys solved the task, not by using abstract, general rules, but by rapidly learning stimulus-response or stimulus-stimulus associations. For example, the monkey could quickly learn an association between a picture of a man on a blue background, and the requirement to release to that same picture when it appears as a test picture, rather than learning that a blue background means "choose same" for all pictures. To test this possibility, we conducted separate behavioral tests after the recording sessions in the PMC, in which new pictures were used on each and every trial. Each monkey was run on a single probe session consisting of 364 trials. During these sessions, the monkeys' performance was virtually identical to that during the recording sessions (monkey A: 89% correct during the probe session vs. 85% correct during the

recording sessions; monkey B: 96 versus 93%), suggesting that the monkeys had indeed learned general, abstract rules rather than specific picture-response associations.

We also examined performance on trials early in the recording session, those in which monkeys saw a given picture for the very first time (i.e., before trial-and-error learning could occur). The monkeys performed significantly above chance (50%) on these trials (67% correct, or 194 correct responses out of a total of 288 pictures [4 pictures \times 72 sessions], $P < 1 \times 10^{-7}$, binomial test). Examining performance across the session, in 100 trial blocks, revealed that the monkeys did not perform as accurately over the first 100 trials as the remainder of the session ($F = 8.2$, $d.f. = 6$, 486, $P < 5 \times 10^{-8}$, one-way ANOVA and post hoc analysis using Bonferroni-corrected t -test; see Fig. 4). This might suggest that they learned additional information over the course of the session (e.g., perhaps they became familiar with the stimuli and were better able to discriminate them). However, across a wide range of cognitive tasks we have found that monkeys typically take a number of trials to perform accurately on any given day. This, coupled with the fact that the monkeys could perform the task just as accurately with trial-unique stimuli, suggests that the most parsimonious explanation is that the monkeys were not using stimulus-response or stimulus-stimulus associations to solve the task.

Neuronal properties

A total of 750 neurons were studied. Some (31) of the neurons were excluded from the analysis because they lay on the boundary of the PMC and PFC (within the arcuate sulcus), and thus could not be accurately ascribed to either area. This left 461 neurons from the PFC (161 from monkey A and 300 from monkey B) and 258 neurons from the PMC (114 from monkey A and 144 from monkey B; see Figs. 2 and 3). Our previous report focused on the activity of the PFC neurons during the sample and the delay epochs (Wallis et al. 2001a). Here, we compare that activity to that of PMC neurons. We also add a detailed examination of activity in the PFC and PMC during the test epoch, which is when the match/nonmatch judgment is made and the behavioral response selected.

To obtain sufficient statistical power, the neurons were pooled across monkeys. For the PFC and PMC comparisons

TABLE 2. Median reaction times (ms) of the two monkeys, across the recording sessions from the two areas and across the different conditions

Rule		Monkey A		Monkey B	
Cue	Response	PFC	PMC	PFC	PMC
"Different" No juice	Release	356	388	389	372
	Hold	324	390	357	357
High tone/green background	Release	389	405	373	356
	Hold	324	423	357	340
"Same" Juice	Release	356	388	408	391
	Hold	324	390	357	373
Low tone/blue background	Release	372	405	372	347
	Hold	307	374	375	359

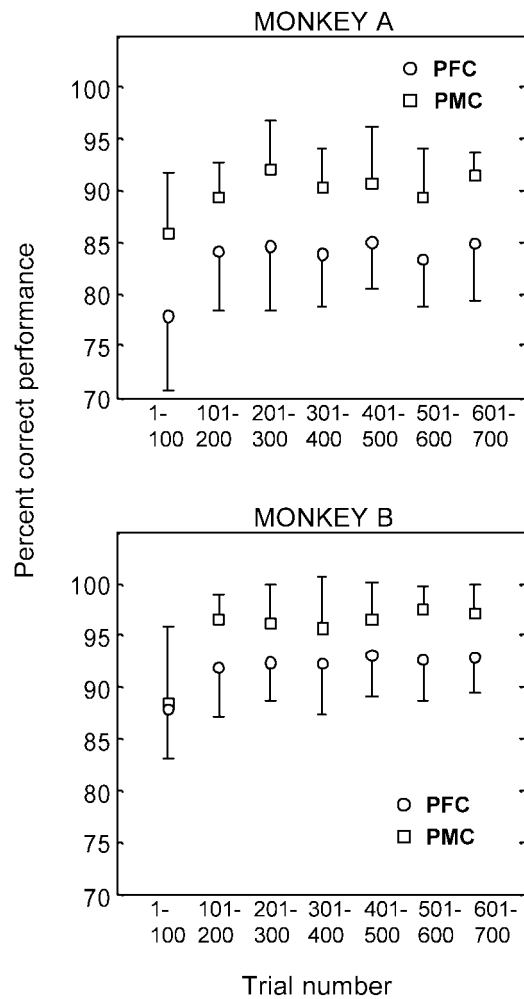


FIG. 4. Behavioral performance across the first 700 trials of recording sessions. Error bars indicate $\pm 1SD$. Both monkeys showed significantly worse performance on the first 100 trials of session.

we made certain that there were no qualitative differences in the data obtained from each monkey individually by ensuring that all main effects were in the same direction in both monkeys and approached significance (assessed as $P < 0.1$). For the comparisons between different PFC regions, or different PMC regions, the smaller sample of neurons precluded such an assessment (given that in each monkey alone the effects may have been nonsignificant, but were significant when pooled) and so we ensured that the effects were at least in the same direction for both monkeys.

Rule selectivity

Figure 5 shows an example of a “rule-selective” PMC neuron: it showed differential activity depending on which rule was currently behaviorally relevant. It had a higher firing rate throughout the trial when the *different* rule was in effect than when the *same* rule was in effect, and this activity was unaffected by which particular cue signaled the rule and which sample picture the monkey was holding in memory.

To examine the time course of the rule effect, we performed a sliding ROC analysis using a 200-ms time window that was incremented across the trial in 10-ms steps (see METHODS). The

result of this analysis for the single rule-selective neuron shown in Fig. 5 is illustrated in Fig. 6. It further demonstrates that this neuron began showing an effect of rule shortly after onset of the rule-signifying cue and then maintained this information throughout the trial until it waned at the end of the test epoch.

We applied this analysis to each and every recorded neuron. The results are shown in Fig. 7A. Plotted are every neuron’s ROC values for every time step. ROC values are derived from the absolute difference in firing rate between *same* rule and *different* rule trials, so every value ranges from 0.5 (no rule information) to nearly 1.0 (perfect discrimination between rules). We sorted the values according to the mean ROC value across the sample, delay, and test epochs. These plots suggest that the effect of rule was stronger, more sustained, and appeared sooner in the PMC than in the PFC. To quantify the strength of the rule effect we also performed an ROC analysis using the mean firing rates of the neurons across the sample epoch and across the delay epoch. This confirmed that rule selectivity was significantly stronger in the PMC than the PFC (Table 3).

We next calculated the latency for the rule effect to appear in neuronal activity after the onset of the rule-signifying cue. To determine latency, we used the sliding ROC analysis, and determined the point at which the ROC values exceeded a threshold of 0.6 for 3 consecutive time bins. The latency was then defined as the center of the first time bin. For the single neuron shown in Fig. 6, the circle at 140 ms indicates the point at which it reached this criterion. During the sample epoch, 114 PFC and 98 PMC neurons reached this criterion. The distributions of the latencies are shown in Fig. 8. It shows that, across this neuron population, rule selectivity appeared significantly earlier in the PMC (median = 280 ms) than in the PFC (median = 415 ms; Wilcoxon’s rank-sum test = 8175, $P < 5 \times 10^{-7}$). This difference was not dependent on the threshold we used for defining the latency. We examined a range of thresholds, from 0.55 to 1.0. For all thresholds ≤ 0.70 , the difference in latencies was significant (at $P < 0.01$), with rule selectivity in the PMC always preceding the PFC (above 0.7, too few neurons reached the criterion to permit a meaningful statistical comparison of the two areas). Despite the fact that the monkeys’ performance during the first 100 trials of the recording session was significantly worse than the remainder of the session (Fig. 4), the strength of rule-selectivity remained constant across the session. We calculated the ROC value in each epoch for 100 trial blocks and found no difference in the ROC values across these blocks in any epoch, or either area ($P > 0.1$ for all comparisons).

Next, we identified neurons that showed significant effects of task variables by applying a 3-way ANOVA to each neuron’s mean firing rate across the sample epoch and across the delay epoch independently (see METHODS). The factors were the current rule, sample picture, and modality of the instructional cue (evaluated at $P < 0.01$). Rule-selective neurons were defined as those that showed a main effect of the rule factor, excluding those neurons that showed a significant interaction with one of the other two factors (see METHODS and below). The results are summarized in Table 4, and show that rule encoding was somewhat more prevalent in the PMC relative to the PFC, although the difference was significant for monkey A only when the data from both monkeys were not pooled.

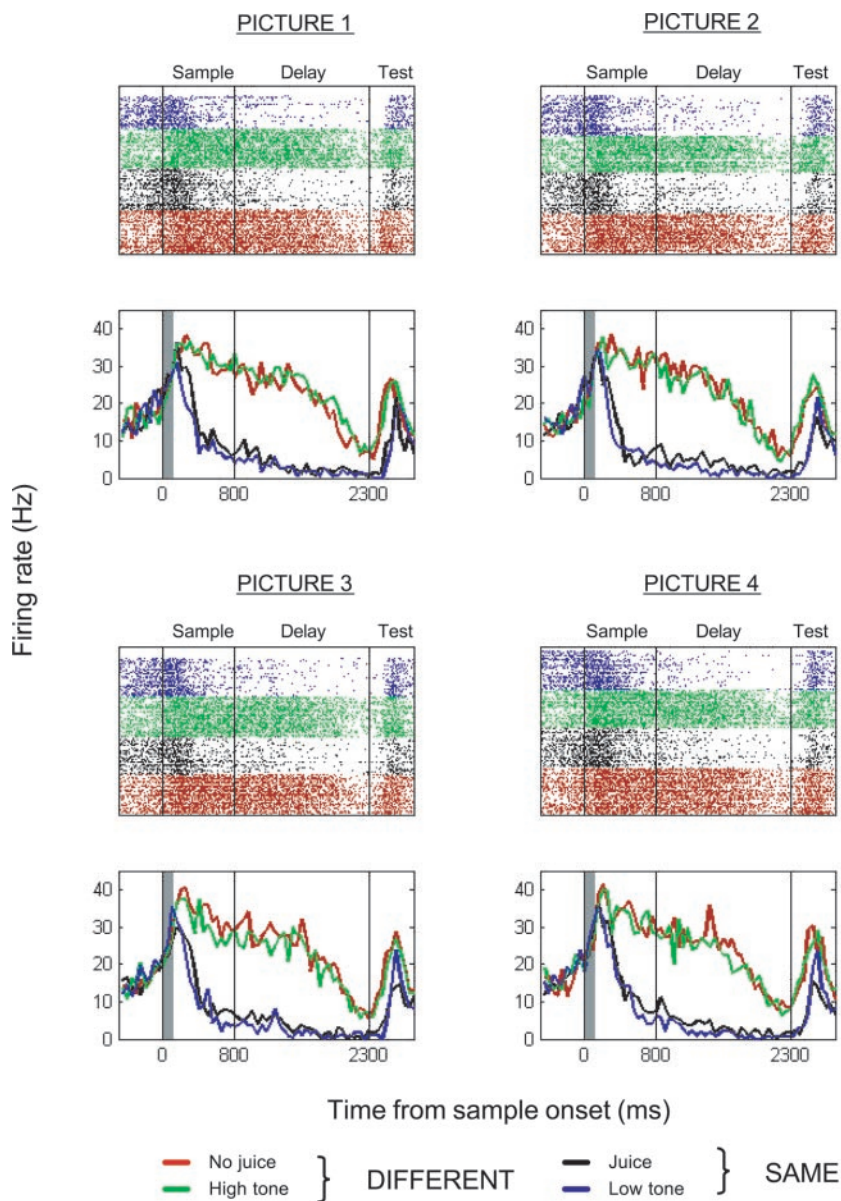


FIG. 5. Raster plots and spike density histograms from a rule-selective neuron recorded from PMC. Simultaneous presentation of the picture and the cue stimulus, which lasted for 100 ms, is shown by the gray bar. This neuron shows a higher firing rate when the *different* rule is in effect, throughout the sample, delay, and test epochs, and a lower firing rate when the *same* rule is in effect. This difference is observed irrespective of whether the cue to signal the rule is a drop of juice or a tone, and irrespective of which of the four pictures is presented.

The rule effect could result from higher activity on *same* rule trials or higher activity on *different* rule trials; we found both types of effects. In the PFC, there was a similar number of neurons that had higher activity to the *different* rule as the *same* rule for both the average sample epoch activity (53/99 or 54% of rule-selective neurons preferred the *different* rule, binomial test, $P > 0.1$) and average delay epoch activity (45/107 or 42% preferred the *different* rule, binomial test, $P > 0.05$). This was also the case for the PMC for the sample epoch (36/67 or 54% of the rule-selective neurons preferred the *different* rule, binomial test, $P > 0.1$), but for average delay epoch activity, there was a significant bias toward PMC neurons showing higher activity to the *different* rule (63/92 or 68%, binomial test, $P < 0.0005$).

Finally, some neurons were most (or least) active after a specific cue, leading to a significant Cue \times Rule interaction in the 3-way ANOVA (see Table 4). This activity could reflect the physical properties of the cue, although, in principle, it could also carry some rule information—for example, by en-

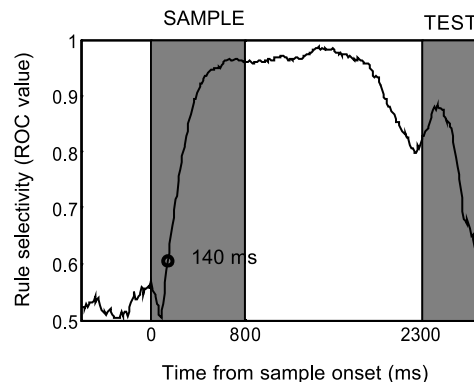


FIG. 6. Results of the sliding ROC analysis performed on the rule-selective neuron shown in Fig. 5. Comparison of the two figures shows that when rule selectivity is most apparent in the spike density histogram (at the end of the sample epoch and throughout most of the delay epoch) the ROC value is correspondingly high. Latency for rule selectivity to appear in this neuron (defined as the point at which the sliding ROC analysis exceeds 0.6 for three consecutive time bins) was calculated as 140 ms, which compares favorably with the value that would be derived by eye from the spike density histogram.

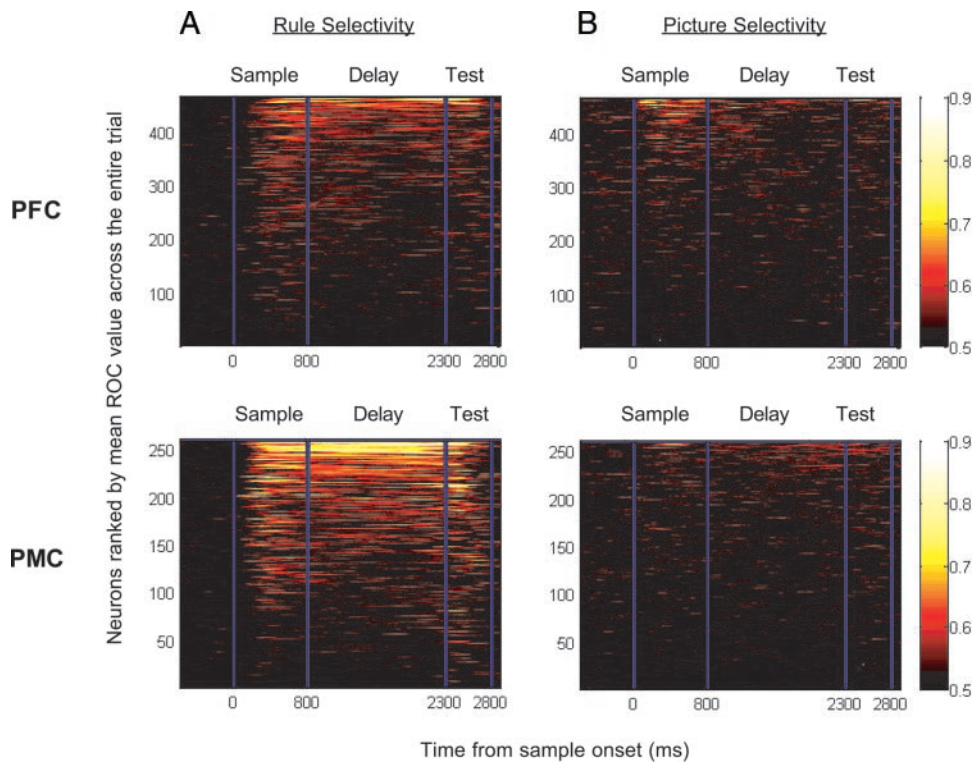


FIG. 7. Time course of rule selectivity (A), and picture selectivity (B), as determined by the sliding ROC analysis, across all neurons from which we recorded. Figures were constructed by sorting neurons according to their mean ROC value across the sample, delay, and test epochs.

coding rule information but only when signaled from a single modality.

Picture selectivity

The requirement to identify and remember the sample picture was also reflected in neuronal activity. An example of a picture-selective PFC neuron is shown in Fig. 9. This neuron did not discriminate between the different rules or cues, but had a higher phasic burst of firing shortly after sample onset for one of the 4 pictures (“sample picture 2”). We used the sliding ROC analysis to examine the time course of picture selectivity for each and every recorded neuron. Overall, picture selectivity was weaker than rule selectivity (Fig. 7B).

We calculated the strength of the picture selectivity by

TABLE 3. Strength of encoding of the different neuronal properties in the PFC and PMC across the sample, delay, and test epochs, as determined by an ROC analysis.

	Epoch	PFC	PMC	P
Rule	Sample	0.537	0.549	<0.0005 ^A
	Delay	0.543	0.574	<1 × 10 ⁻¹¹
Picture	Sample	0.537	0.532	<0.005
	Delay	0.532	0.533	>0.1
	Test	0.542	0.532	<0.00001
Match/Non-match	Test	0.523	0.523	>0.1
Behavioral response	Test	0.537	0.572	<5 × 10 ⁻¹⁵

The figures are the median ROC values across all the neurons from which we recorded. All of the ROC values are significantly different from chance, as determined by a bootstrap analysis (see METHODS). Picture selectivity in the sample and delay epochs was measured with respect to the sample picture, and in the test epoch was measured with respect to the test picture. The P value relates to the difference between areas determined using a Wilcoxon’s rank-sum test. The superscript A indicates that the difference was significant in monkey A only when the data were not pooled.

computing an ROC value using the mean firing rate of each neuron across the sample and delay epochs. We compared activity to each neuron’s “preferred” picture (the picture that elicited the highest mean firing rate in the neuron) and “non-preferred” picture (the picture that elicited the lowest mean firing rate). There was a weak tendency for picture selectivity

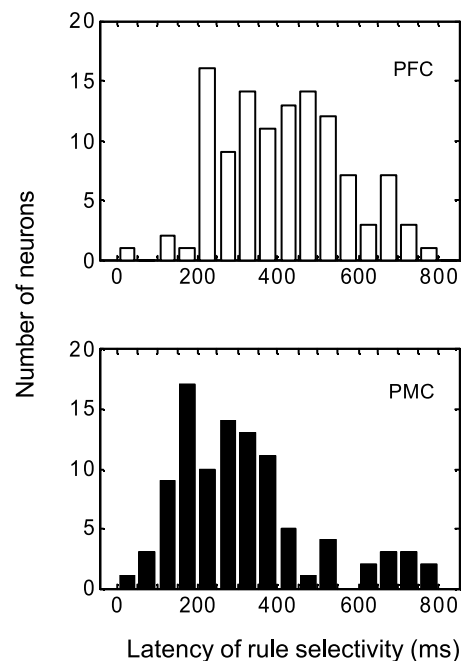


FIG. 8. Distribution of latencies for rule selectivity to appear in neuronal activity, across all neurons from which we recorded, as determined by the sliding ROC analysis. Latency was defined as the point at which the sliding ROC analysis exceeded 0.6 for three consecutive 10-ms time bins. The PMC distribution is shifted to the left of the PFC distribution, reflecting a median onset in PMC of 280 ms, compared with 415 ms in PFC.

TABLE 4. Percentage of neurons that were selective to the cue, the rule, or the sample picture that was presented, during either the sample epoch or delay epoch

Percentage of Cells With Main Effect of:	Sample			Delay		
	PFC	PMC	<i>P</i>	PFC	PMC	<i>P</i>
Cue	17	12	>0.05	11	16	>0.01
Rule	21	26	>0.1	23	36	<0.001 ^A
Sample picture	12	3	<0.0005 ^A	6	3	>0.05
Cue × Rule	21	32	<0.001 ^A	15	31	<5 × 10 ⁻⁸
Rule × Sample picture	1	0	>0.1	0	0	>0.1
Cue × Sample picture	1	1	>0.1	2	2	>0.1

PFC *N* = 461, PMC *N* = 258. Selectivity was defined using a 3-way ANOVA (see METHODS). Significant differences were determined using a chi-square test. The superscript A indicates that the difference was significant in monkey A only when the data were not pooled.

to be stronger in the PFC than in the PMC during the sample epoch (Table 3). We also compared the incidence of neurons whose mean sample and/or delay epoch activity was picture selective according to the 3-way ANOVA (described above, assessed at *P* < 0.01). This revealed a weak tendency toward

more PFC neurons showing significant effects, but only in the sample epoch, and the difference was significant in monkey A only when the data from both monkeys were not pooled (Table 4).

We calculated the latency for picture selectivity to appear in

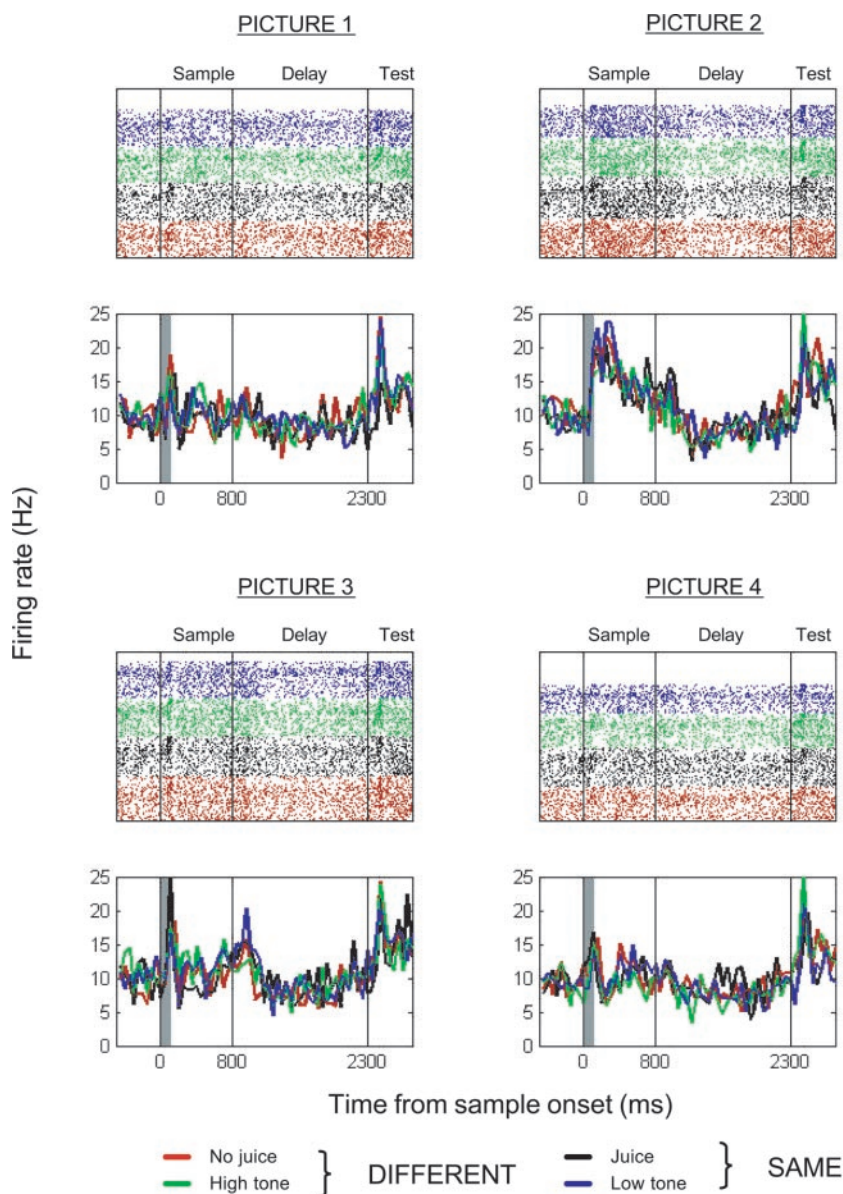


FIG. 9. Raster plots and spike density histograms from a picture-selective neuron recorded from PFC. Simultaneous presentation of the picture and cue stimulus, which lasted for 100 ms, is shown by the gray bar. This neuron shows differential activity during the sample epoch, depending on which picture is presented as the sample stimulus. The neuron shows a phasic increase in activity when picture two is presented, as opposed to a decrease in activity when any of the other three pictures is presented, but does not discriminate between rules, or cues that signal rules.

neuronal activity after the sample onset using the sliding ROC values and the same criterion as we did for rule selectivity (3 consecutive 10-ms time steps where the ROC value exceeded 0.6; see above and METHODS). During the sample epoch, 76 PFC neurons and 11 PMC neurons reached this criterion. The low number of PMC neurons that reached criterion precluded a meaningful statistical comparison of the latencies, although the median latency for picture selectivity to appear in the PFC (median 205 ms) was earlier than in the PMC (median 390 ms).

We also examined picture selectivity for the test stimulus that appeared at the end of the trial. The sliding ROC analysis for all recorded neurons (see above and METHODS) is pictured in Fig. 10A. It suggests stronger test picture selectivity in the PFC than in the PMC, just as we found for the sample picture. This was confirmed by performing an ROC analysis comparing the neuron's mean activity to its "preferred" and "nonpreferred" test pictures (see Table 3). We also identified neurons selective for the test picture through a Kruskal–Wallis one-way ANOVA on the average test epoch activity using the 4 different test pictures as a factor (assessed at $P < 0.01$). This revealed that more neurons in the PFC (106/461 or 23%) than in the PMC (10/258 or 4%) were test picture selective (chi-square = 43.3, $d.f. = 1$, $P < 5 \times 10^{-12}$).

Selecting the behavioral response: activity during the test epoch

When the test picture was presented, monkeys needed to determine whether it matched the sample picture and then choose the appropriate behavioral response (hold or release) depending on the match/nonmatch status of the test picture and the current rule. So, we looked for their neuronal correlates during the test epoch.

Some neurons showed an effect of the match/nonmatch status of the test picture. An example of a single PFC neuron is shown in Fig. 11A. It showed higher activity to matches than

to nonmatches, largely irrespective of which behavioral response the match or nonmatch required. Figure 10B shows the sliding ROC analysis of the match/nonmatch effect (see above and METHODS) for all recorded neurons. Although the match/nonmatch effect appeared to be somewhat stronger in some of the PFC neurons than in the PMC neurons, an ROC analysis on the average activity across the test epoch did not reveal a significant difference between the strength of this effect between the entire PFC and PMC neuronal populations (Table 3). The latency for the match/nonmatch effects (defined as the point at which the sliding ROC analysis exceeded 0.6 for 3 consecutive time bins) also did not differ between the 2 areas (PFC median latency = 290 ms, $n = 19$, PMC median latency = 325 ms, $n = 8$, Wilcoxon's rank-sum test = 137, $P > 0.1$), although the test was underpowered because of the small number of neurons reaching the criterion.

We also identified neurons with match/nonmatch effects using a Wilcoxon's rank-sum test (assessed at $P < 0.01$) that compared average test epoch activity on match versus nonmatch trials. This revealed that a similar proportion of neurons in the PFC (63/461 or 14%) and the PMC (27/258 or 10%; chi-square = 1.3, $d.f. = 1$, $P > 0.1$) showed a significant effect. In the PFC, the majority of neurons with a match/nonmatch effect showed higher activity to nonmatches than to matches (45/63, or 71%, binomial test, $P < 0.0005$). There was no such bias in the PMC: 13/27 or 48% of the neurons with a match/nonmatch effect had a higher firing rate to nonmatching test pictures, a proportion that did not significantly differ from 50% (binomial test, $P > 0.1$).

Some of the neurons that showed a significant match/nonmatch effect also encoded the current rule during the delay epoch that preceded the test picture (according to the 3-way ANOVA described above). An example of a PFC neuron with this property is shown in Fig. 11B. It reflected the rule during the delay epoch (it had higher activity when the *different* rule

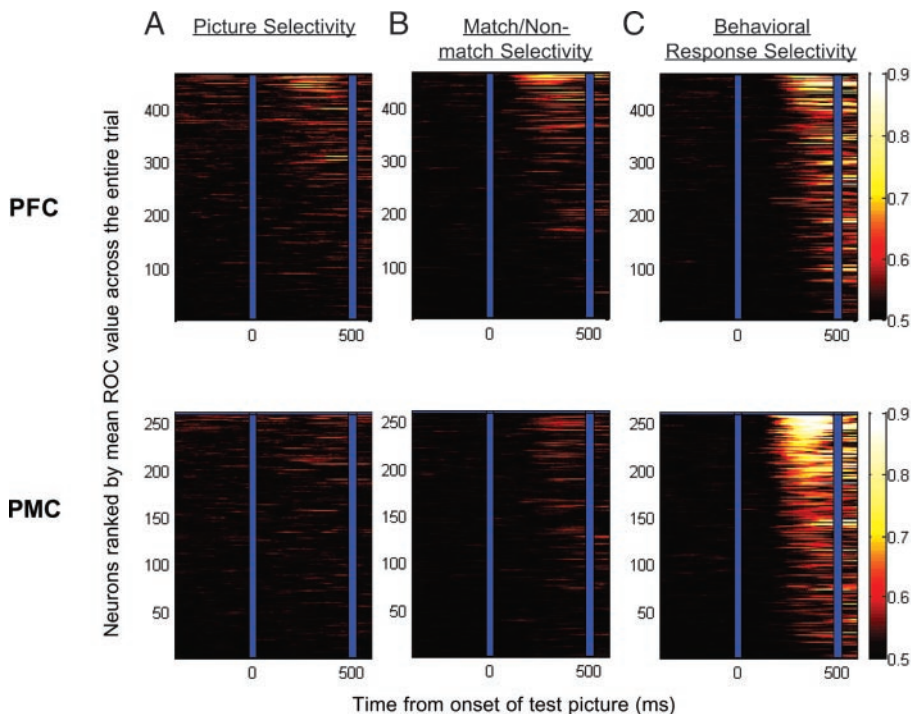


FIG. 10. Time course of picture selectivity (A), the match/nonmatch effect (B), and the encoding of the behavioral response (C) as determined by the sliding ROC analysis, across all neurons from which we recorded. Figures were constructed by sorting neurons according to their mean ROC value across the sample, delay, and test epochs.

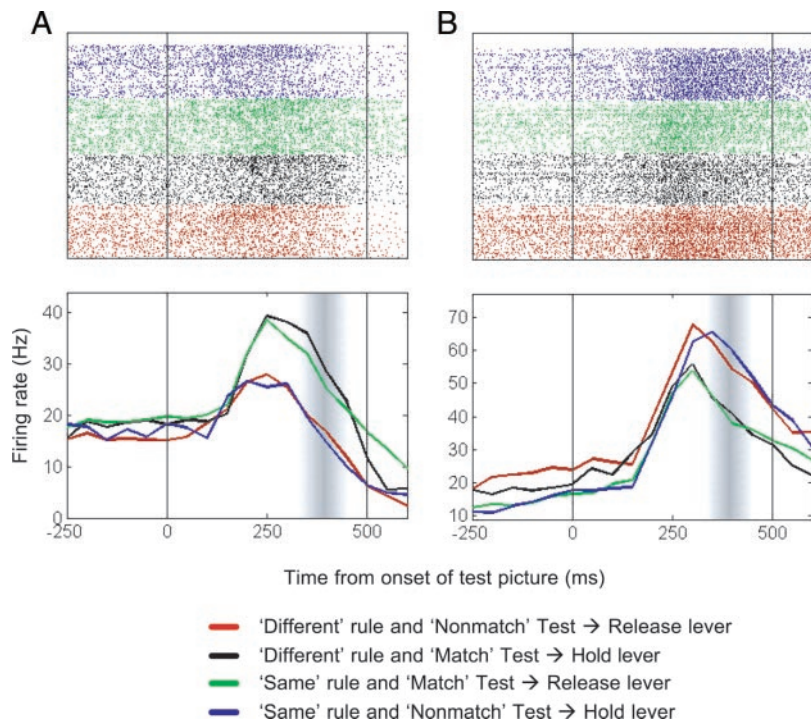


FIG. 11. *A*: PFC neuron that has a higher firing rate when the test picture matches the sample picture. *B*: PFC neuron that initially encodes the *different* rule, but then switches to encode whether the test picture matches the sample picture. Each graph illustrates the last 250 ms of the delay epoch and the entire 500-ms test epoch. Gray bar: mean reaction time of monkey on “release” trials, $\pm 1SD$.

was in effect) but shortly after the onset of the test picture, its selectivity changed to reflect the match/nonmatch status of the test picture (it showed higher activity when the test picture was a nonmatch) and no longer reflected the current rule. The proportion of neurons encoding the match/nonmatch status of the test picture that also encoded the rule was not significantly different between the areas (PFC: 14/63 or 22%; PMC: 11/27, or 41%; chi-square = 2.4, *df* = 1, *P* > 0.1).

Next, we examined neurons whose activity reflected the behavioral response. An example of a PMC neuron showing

this effect is illustrated in Fig. 12*A*. This neuron had a higher test epoch firing rate on trials when the monkey released the lever as opposed to those trials when the monkey held the lever, irrespective of which combination of rule and test picture match/nonmatch status cued that response. The sliding ROC analysis (Fig. 10*C*; see METHODS and above) on all recorded neurons revealed that the behavioral response was apparent in both PFC and PMC neuronal activity. However, it seemed to appear sooner and was stronger in the PMC. An ROC analysis comparing average test epoch activity for each neuron on trials

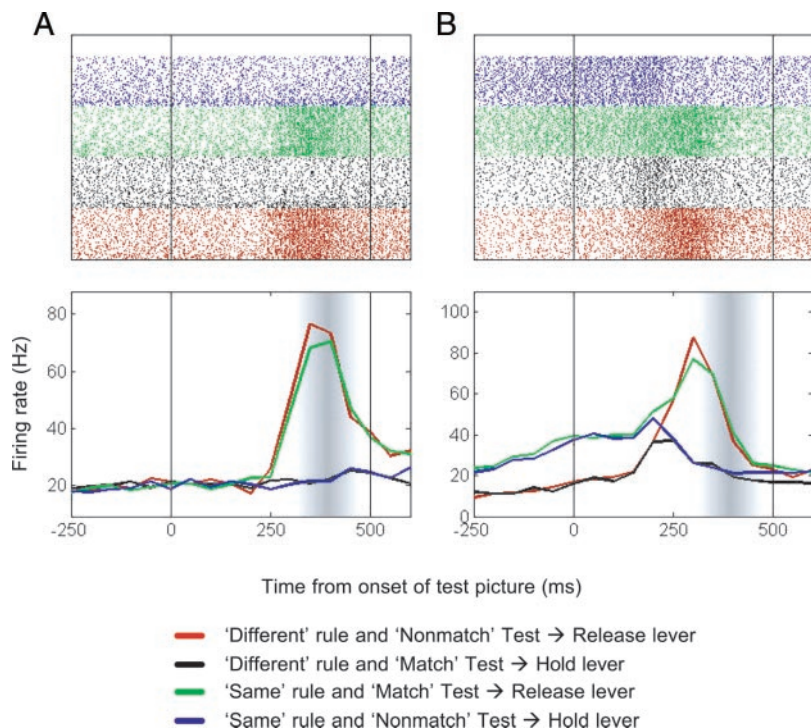


FIG. 12. *A*: PMC neuron encoding the behavioral response; this cell has a higher firing rate when the correct response is to release the lever. *B*: PMC neuron that initially encodes the *same* rule, but then switches to encode the behavioral response. Each graph illustrates the last 250 ms of the delay epoch and the entire 500-ms test epoch. Gray bar: mean reaction time of monkey on “release” trials, $\pm 1SD$.

when the monkey held versus released the lever revealed that the effect of the behavioral response was indeed stronger in the PMC (Table 3).

In the sliding ROC analysis pictured in Fig. 10C, behavioral-response selectivity appeared to arise earlier in the PMC than in the PFC. To confirm this, we computed the latency for selectivity for each neuron (defined as the point at which the sliding ROC analysis exceeded 0.6 for 3 consecutive time bins, as above; also see METHODS). During the test epoch, 128 PFC and 134 PMC neurons reached this criterion. Selectivity for the behavioral response appeared significantly earlier in the PMC population (median latency = 270 ms) than the PFC population (median = 330 ms, Wilcoxon's rank-sum test = 20,255, $P < 5 \times 10^{-8}$; see Fig. 13). This difference in latencies was not dependent on the threshold that we used. All thresholds from 0.55 to 0.80 produced a significant difference between the two areas in the distribution of latencies, and in all cases the PMC encoded the behavioral response before the PFC.

We also identified neurons that showed an effect of behavioral response using Wilcoxon's rank-sum test (assessed at $P < 0.01$) on average test epoch activity. Such behavioral response-selective neurons were significantly more prevalent in the PMC (170/258 or 66%) than in the PFC (159/461 or 35%; chi-square = 64.5, $d.f. = 1$, $P < 1 \times 10^{-16}$). In the PFC, there was an even split between the selective neurons that had a higher firing rate on release trials (87/159 or 55%) and those that had a higher firing rate on hold trials (72/159 or 45%, binomial test, $P > 0.1$). In the PMC, however, more behavioral response-selective neurons had higher activity on release trials (102/170

or 60%, binomial test, $P < 0.01$) than on hold trials. Many of these neurons also reflected the rule during the preceding delay epoch. For example, the neuron in Fig. 12B has a higher firing rate on *same* rule trials as opposed to *different* rule trials during the delay. However, about halfway through the test epoch, its activity switched; it then reflected the behavioral response (with more activity on release trials) and no longer reflected the rule. Similar numbers of behavioral response-selective PFC (46/159 or 29%) and PMC (62/170 or 36%) neurons also encoded the rule during the delay epoch (chi-square = 1.8, $d.f. = 1$, $P > 0.1$).

Both monkeys held and released the lever with their left hand. However, there was no difference in the incidence of neurons encoding the behavioral response between the two cerebral hemispheres. In the PFC, 120/326 (37%) of the neurons recorded in the right hemisphere reflected the behavioral response compared with 39/135 (29%) of the neurons recorded in the left hemisphere (chi-square = 0.28, $d.f. = 1$, $P > 0.1$). In the PMC, 123/180 (68%) of neurons in the right hemisphere reflected the response compared with 47/78 (60%) in the left hemisphere (chi-square = 0.05, $d.f. = 1$, $P > 0.1$).

Comparison to behavioral performance

The main difference we observed between the two areas was a stronger and earlier encoding of both the rule and the behavioral response in the PMC relative to the PFC. However, the monkeys' performance was also better when we recorded from the PMC versus the PFC. To ensure that this did not account for the differences in neuronal activity, we ranked the recording sessions in terms of performance for each monkey, and compared the more poorly performed half of the PMC sessions to the better-performed half of the PFC sessions. There was no difference in the monkeys' performance between these two groups of sessions (PFC: 90%, $n = 29$, PMC: 91%, $n = 9$, Wilcoxon's rank-sum test = 202, $P > 0.1$).

Our analysis of this reduced data set revealed that the PMC still encoded the rule before the PFC (median PFC latency = 420 ms, $n = 73$, median PMC latency = 270 ms, $n = 51$, Wilcoxon's rank-sum test = 2,283, $P < 5 \times 10^{-6}$), as well as the behavioral response (median PFC latency = 355 ms, $n = 66$, median PMC latency = 380 ms, $n = 76$, Wilcoxon's rank-sum latency = 4,530, $P < 1 \times 10^{-6}$). The rule selectivity was also stronger in the PMC than in the PFC during the delay epoch (median ROC value in the PFC = 0.541, $n = 264$, median ROC value in the PMC = 0.578, $n = 143$, Wilcoxon's rank-sum test = 35229, $P < 1 \times 10^{-7}$), although with the reduced data set the difference between the areas did not reach significance during the sample epoch (median ROC value in the PFC = 0.536, $n = 264$, median ROC value in the PMC = 0.548, $n = 143$, Wilcoxon's rank-sum test = 31,607, $P > 0.01$). Finally, selectivity for the behavioral response was also still stronger in the PMC than in the PFC (median ROC value in the PFC = 0.535, $n = 264$, median ROC value in the PMC = 0.571, $n = 143$, Wilcoxon's rank-sum test = 36,233, $P < 5 \times 10^{-10}$).

Comparison of "switch" and "stay" trials

The impairments that patients with PFC damage exhibit on rule-following tasks are most profound when the patient is

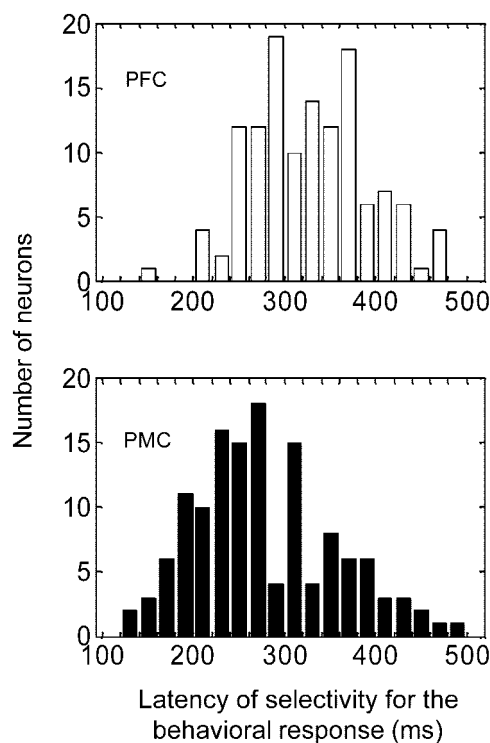


FIG. 13. Distribution of latencies for selectivity relating to behavioral response to appear in neuronal activity, across all neurons from which we recorded, as determined by the sliding ROC analysis. Latency was defined as the point at which the sliding ROC analysis exceeded 0.6 for three consecutive 10-ms time bins. The PMC distribution is shifted to the left of the PFC distribution, reflecting a median onset in PMC of 270 ms, compared with 330 ms in PFC.

required to switch from one rule to another. This phenomenon is termed “perseveration” (Milner 1963; Nelson 1976; Owen et al. 1991; Stuss et al. 2000). In our task, the rules varied randomly from trial to trial. Thus there was no discrete point at which monkeys had to switch from a currently familiar rule to a new one. Nonetheless, we compared the monkeys’ behavior and rule-related activity from trials when the rule had switched from the previous trial (“switch” trials) to that from trials when the rule was the same as the previous trial (“stay” trials).

There was no difference between the monkeys’ level of performance on switch trials and stay trials (switch trials: 89%; stay trials: 88%), and no difference in their median behavioral reaction times (373 ms for both types of trials). Accordingly, we also found that neural activity was largely similar between these trials.

To examine rule selectivity between stay and switch trials, we computed ROC values using each neuron’s average activity across the sample epoch and across the delay epoch (see METHODS). During the sample epoch, neither PFC nor PMC neurons showed a difference in magnitude of rule selectivity between stay and switch trials (PFC neurons: median ROC value on “same” trials = 0.543, median ROC value on “switch” trials = 0.542, Wilcoxon’s matched-pairs signed-ranks test = 52,054, $n = 461$, $P > 0.1$; PMC neurons: median ROC value on “same” trials = 0.554, median ROC value on “switch” trials = 0.555, Wilcoxon’s matched-pairs signed-ranks test = 50,708, $n = 258$, $P > 0.1$). During the delay epoch, there was no difference in magnitude of rule effect between switch and stay trials for the PFC neurons (median ROC value on “same” trials = 0.548, median ROC value on “switch” trials = 0.544, Wilcoxon’s matched-pairs signed-ranks test = 14,824, $n = 461$, $P > 0.1$). However, in the PMC there was a slightly, but significantly, higher value on “switch” trials (median ROC value on “same” trials = 0.570, median ROC value on “switch” trials = 0.578, Wilcoxon’s matched-pairs signed-ranks test = 12,503, $n = 258$, $P < 0.001$). This may be attributed to the fact that significantly more PMC neurons (154/258 or 60%) showed stronger selectivity on “switch” trials than on “same” trials (binomial test, $P < 0.00005$). To examine the time course of rule selectivity on “switch” versus “stay” trials, we performed a sliding ROC analysis (as above and see METHODS) but there were no differences in the latency of selectivity on these two types of trial in either area ($P > 0.1$ in all cases).

Prefrontal regional specialization: neuronal properties of three prefrontal subregions

We recorded neural activity over a wide expanse of the PFC, which afforded an opportunity to examine whether there was any regional specificity of neuronal properties (Figs. 2 and 3). We compared 3 major PFC subregions: the dorsolateral prefrontal cortex (DLPFC, defined as the cortex dorsal to the ventral lip of the principal sulcus), the ventrolateral PFC (VLPFC, defined as the cortex from the ventral lip of the principal sulcus to the lateral lip of the lateral orbital sulcus), and the orbitofrontal cortex (OFC, defined as the cortex medial to the lateral lip of the lateral orbital sulcus). We used the same analyses that we had used to compare the PFC and the PMC to examine the incidence, strength of encoding and latency of the different neuronal properties.

We previously reported (Wallis et al. 2001a) that there were more neurons in the VLPFC than in the DLPFC and the OFC whose activity varied significantly with sample picture and that rule-selective neurons were equally distributed throughout all 3 areas. An analysis of test epoch activity also revealed regional differences. In the VLPFC, 65/175 (38%) of neurons were selective for the identity of test picture (as determined by a Kruskal–Wallis ANOVA), compared with 17/182 (12%) of neurons in the DLPFC and 24/104 (23%) of neurons in the OFC (chi-square = 37.4, $d.f. = 2$, $P < 1 \times 10^{-9}$). A post hoc analysis, using multiple chi-square tests and a Bonferroni-corrected alpha level of 0.0033, showed that the incidence of picture-selective neurons in the DLPFC was significantly lower than the incidence in either the VLPFC ($P < 1 \times 10^{-10}$) or the OFC ($P < 0.0033$). The incidence of picture selectivity in the VLPFC and OFC did not significantly differ ($P > 0.01$). There was also a difference between the areas in the incidence of neurons encoding the match/nonmatch status of the test pictures, as revealed by Wilcoxon’s rank-sum tests on each neuron’s average activity across the test epoch (VLPFC 39/175 or 22%, DLPFC 11/182 or 6%, OFC 13/104 or 13%; chi-square = 18.7, $d.f. = 2$, $P < 0.0001$). Post hoc analysis revealed that the incidence of such neurons in the VLPFC was higher than that in the DLPFC ($P < 0.00005$), whereas the incidence in the OFC did not differ from either the VLPFC ($P > 0.05$) or the DLPFC ($P > 0.05$). Finally, there was not a significant difference in the incidence of neurons that reflected the behavioral response, as determined by a Wilcoxon’s rank-sum test on average activity across the test epoch (DLPFC 49/182 or 26%, VLPFC 64/175 or 38%, OFC 46/104 or 47%, chi-square = 8.48, $d.f. = 2$, $P > 0.01$).

With regard to the strength of the encoding (as determined by an ROC analysis on each neuron’s average test epoch activity) there was a bias for VLPFC neurons, relative to DLPFC and OFC neurons, to show a stronger effect of the identity of the sample picture (during the sample epoch) and the test picture (during the test epoch) and of the match/nonmatch status of the test picture (Table 5). During the sample epoch, there was also a tendency for the DLPFC to

TABLE 5. *Strength of encoding of the different neuronal properties in the different subregions of the PFC across the sample, delay, and test epochs, as determined by ROC analysis*

	Epoch	DLPFC	VLPFC	OFC	<i>P</i>	Post hoc
Rule	Sample	0.545	0.542	0.526	<0.01	D vs.O
	Delay	0.550	0.543	0.534	>0.01	—
Picture	Sample	0.534	0.544	0.535	<0.0005	V vs.O
	Delay	0.528	0.542	0.528	<0.005	V vs.D V vs.D
Match/ non-match	Test	0.540	0.550	0.534	<0.0001	V vs.O V vs.D
	Test	0.519	0.528	0.519	<0.001	V vs.O
Behavioral response	Test	0.534	0.538	0.544	>0.01	—

The figures are the median ROC values across all the neurons from which we recorded. All of the above ROC values are significantly different from chance, as determined by a bootstrap analysis, except for the values in italics (see METHODS). Picture selectivity in the sample and delay epochs was measured with respect to the sample picture, and in the test epoch was measured with respect to the test picture. The *P* value relates to the difference between areas determined using a Wilcoxon’s rank-sum test.

encode the rule more strongly than in the OFC, and during the delay epoch the VLPFC encoded the identity of the sample picture more strongly than in the DLPFC, but not the OFC. The only difference in latencies among the 3 areas was a slight tendency for the OFC to encode the rule earlier than the DLPFC (median DLPFC latency = 585 ms, $n = 40$, VLPFC = 480 ms, $n = 51$, OFC = 370 ms, $n = 19$, Kruskal–Wallis one-way ANOVA, chi-square = 14.9, $d.f. = 2,107$, $P < 0.001$).

PMC regional specializations

In comparison to our recordings from the PFC, the PMC recordings were restricted to a smaller cortical area. The area we recorded from was bounded by the superior arcuate sulcus and the arcuate sulcus spur at its ventral extent, the end of the arcuate sulcus spur at the posterior extent, and the superior precentral dimple at the dorsal extent (Figs. 2 and 3). The recordings extended no further than 5 mm anterior to the genu of the arcuate sulcus, dorsal and superior to the superior limb of the arcuate sulcus. The recording locations were intended to match those of previous studies that have compared neuronal properties in the PFC and PMC (di Pellegrino and Wise 1991, 1993), and as such the recordings were largely restricted to area F2 (Matelli et al. 1985).

Within this area neuronal properties were largely homogeneous, although there was a slight clustering of neurons that were rule selective during the delay in the more posterior extent of the recording area. To quantify this effect we compared the incidence of selective neurons anterior to the genu of the arcuate sulcus ($n = 128$) to those posterior to the genu ($n = 130$).

There were no differences in the distribution of neurons that showed a significant rule effect in their average activity across the sample epoch according to the 3-way ANOVA (posterior PMC: 41/130 or 32%, anterior PMC: 25/128 or 20%; chi-square = 4.27, $d.f. = 1$, $P > 0.01$). For the delay epoch, however, the posterior PMC had a greater proportion of neurons that were rule selective (57/130 or 44%) than in the anterior PMC (34/128 or 27%, chi-square = 7.70, $d.f. = 1$, $P < 0.01$). Furthermore, the rule was more strongly encoded in the posterior PMC during both the sample epoch (median ROC value in posterior PMC = 0.568, median ROC value in anterior PMC = 0.538, Wilcoxon's rank-sum test = 14083, $P < 0.00005$) and the delay epoch (median ROC value in posterior PMC = 0.612, median ROC value in anterior PMC = 0.554, Wilcoxon's rank-sum test = 13498, $P < 5 \times 10^{-7}$).

During the test epoch, there was no difference in the incidence of neurons encoding the identity of the test picture (posterior PMC: 7/130 or 5%, anterior PMC: 3/128 or 2%, chi-square = 0.88, $d.f. = 1$, $P > 0.1$), its match/nonmatch status (posterior PMC: 17/130 or 13%, anterior PMC: 10/128 or 8%, chi-square = 1.38, $d.f. = 1$, $P > 0.1$), or the behavioral response (posterior: 90/130 or 69%, anterior: 80/128 or 63%, chi-square = 1.02, $d.f. = 1$, $P > 0.1$). However, the behavioral response was encoded more strongly in average test epoch activity in the posterior PMC (median ROC value = 0.599) compared with that in the anterior PMC (median ROC value = 0.563, Wilcoxon's rank-sum test = 14,481, $P < 0.0005$).

Finally, there were no significant differences between the

two regions in the latency to encode any of the above information ($P > 0.1$ in all cases).

DISCUSSION

This study compared and contrasted neuronal correlates of rule-guided actions in the PFC and PMC. First and foremost, our results indicate a large degree of overlap in the neuronal properties of the PFC and PMC. All the relevant features of the task (the identities of the pictures, the current rule, the match/nonmatch status of the test picture, and the behavioral response) were reflected in each area's neuronal activity. This argues against a strict compartmentalization of function between the areas, at least for the mechanisms investigated here.

At the same time, however, there was evidence for some degree of specialization: there were differences in the incidence, strength, and latency of effects. Encoding of both the rule and the behavioral response occurred earlier and was stronger and more abundant in the PMC than PFC. In contrast, the PFC contained some neurons that encoded picture identity, but they were rare in the PMC.

Below, we discuss these results in more detail.

Abstract rules

The abstraction of higher-order rules permits a shortcut in an organism's learning. It is a form of generalization that allows the organism to maximize flexibility and the amount of reward. For example, the monkey could have potentially solved our task quickly learning, on each day, a set of 16 associations (4 pictures \times 4 cues). The monkey might learn that picture A on a blue background is associated with picture A (*same*), whereas picture A on a green background is associated with anything but picture A (*different*). This is inefficient because learning these associations tells nothing about the correct response to picture B on a blue background. Unless the monkey extracts a general rule that a blue background means "same," it would have to learn 16 new associations by trial and error each day, wasting many reward opportunities through error. Our monkeys apparently did make this abstraction; they performed well above chance when viewing pictures for very first time and could even perform the task with a new picture on every single trial.

The economy that this abstraction permits was reflected in the neural activity. It would have been possible to solve the task without abstracting the rule on the single neuron level. For example, there could have been two populations of neurons, one for encoding the rules when instructed by one modality (e.g., vision) and another population when they are instructed in another modality (e.g., taste). However, if another cue modality were introduced, a third population of neurons would then be needed. Whether on the behavioral or neural level, abstracting the rules beyond sensory details allows them to be quickly and efficiently generalized to novel circumstances.

Rule- and response-encoding in the PFC versus PMC

Deficits in switching between different abstract rules are a cardinal feature of PFC damage (Milner 1963; Nelson 1976; Owen et al. 1991; Stuss et al. 2000) and we have previously reported an abundance of PFC neurons that encoded the rules used here (Wallis et al. 2001a). However, we now report that

rule (and response-related) signals were even stronger and appeared earlier in the PMC than in the PFC, which suggests a greater role for the PMC in encoding them. This may be because the rules were highly familiar; monkeys practiced this task for many thousands of trials. In both humans and monkeys, PFC damage preferentially affects new learning; they can still engage in complex behaviors as long as they were well learned before the damage (Dias et al. 1997; Knight 1984; Shallice 1982; Shallice and Evans 1978). Further support for this comes from observations that PFC neurons are more strongly activated during new learning than during the performance of a familiar task (Asaad et al. 1998) and imaging studies that report a decrease in blood flow to the PFC as a task becomes more familiar and routine (Raichle et al. 1994). It may be that the PFC plays a greater role in rule acquisition but then, with increasing practice, the task becomes more strongly encoded in “downstream” motor system structures (Wise et al. 1996). This is consistent with Fuster’s (1997) multilevel perception–action hierarchy; the PFC is at the apex, but the sensory-to-motor transformations can occur at lower levels (e.g., the PMC) with relatively simple and/or highly familiar behaviors. Further support for this notion comes from an event-related fMRI study in which a region of cortex at the junction of areas 44, 8A, and 6 (Petrides and Pandya 1994) had increased blood flow during the performance of the Wisconsin Card Sorting Test, a test that requires the subject to switch between sorting cards according to different abstract rules (Monchi et al. 2001). Unlike more anterior prefrontal regions, which were active only when the rule switched, this region was also active when the patients were sorting according to an established rule. The authors concluded that the area may be responsible for the selection of the appropriate response according to the current rule, rather than initially establishing the rule, a conclusion that is consistent with our results. Finally, it is also important to note that in patient studies that have associated the PFC with rule-based behaviors, damage often encroaches into the PMC. As such, it is unclear whether the PMC might contribute to them.

Many previous studies investigating the neuronal properties of the lateral PMC have focused predominantly on encoding of a specific motor response (e.g., Kalaska and Crammond 1995; Weinrich and Wise 1982; Weinrich et al. 1984), set-related activity (neurons that encode a forthcoming response; e.g., Godschalk et al. 1985; Weinrich et al. 1984; Wise and Mauritz 1985), or the learning and processing of conditional motor associations (Mitz et al. 1991). Our results do not contradict such studies because we found many neurons in the PMC that encoded the behavioral response. However, they suggest the PMC is also capable of representing actions at a higher-order, more abstract level than specific movements or responses.

Perceptual and motor biases within the frontal lobe

More neurons in the PFC than in the PMC encoded the identity of the sample and test pictures, suggesting a perceptual bias in the neuronal properties of the PFC relative to those of the PMC. This conclusion is consistent with other studies investigating the neuronal properties of the PFC (Boussaoud and Wise 1993a; Constantinidis et al. 2001; Funahashi et al. 1989). There was also a bias toward encoding of the picture identity in the ventrolateral PFC, relative to other PFC regions,

in accord with our previous findings (Wallis et al. 2001a), as well as a bias for the ventrolateral PFC to encode the match/nonmatch status of the test picture relative to other PFC regions. These results make sense, given that the ventrolateral PFC is preferentially connected to the inferotemporal cortex (ITC) (Carmichael and Price 1995), an area known to encode the identity of objects (Gross 1994). Furthermore, ITC neurons also show match/nonmatch effects (Miller et al. 1993), although some degree of interaction with the PFC is probably necessary for this judgment because such neurons are more common in the PFC than in the ITC (Miller et al. 1996).

By contrast, the PMC had a clear motor bias relative to the PFC. More PMC neurons encoded the behavioral response and their selectivity was stronger and appeared earlier than in the PFC. Previous studies have also found that many PFC neurons reflect forthcoming behavioral responses (Asaad et al. 1998; Fuster et al. 1982; Kubota and Funahashi 1982; Niki 1974a–c). An implication (and common assumption) of the frontal hierarchy is that motor-related activity in the PFC amounts to commands that drive activity in downstream motor structures, such as the PMC and the primary motor cortex, which in turn translate the command into a movement. Our results show that this is not always the case; on average motor signals appeared 60 ms earlier in the PMC than in the PFC. In fact, because PFC neurons do not begin to encode the behavioral response until after PMC neurons, it may be that the PFC does not directly participate in the selection of the response, but rather receives an “efference copy” of it.

Interpretational issues

The latency differences that we observed between the PFC and PMC in encoding the rule and the behavioral response were large (135 and 60 ms, respectively), particularly when one considers that these two areas are separated by as little as one synapse. In making these comparisons between the two areas, it is important not to introduce any spurious bias. Thus we did not preselect neurons based on responsiveness or selectivity, during either recording or analyzing the data, and so we often included neurons that showed little or no selectivity to the task conditions of interest. This reduced the size of the effects that we observed when considering the overall neuronal population (e.g., Table 3), and raised the possibility that we would have observed different effects had we focused on those neurons with the strongest representation of the task. However, there was no evidence that this was the case. The latency differences were consistent across the criterion’s wide range; increasing the criterion so that the analysis was restricted to those neurons that showed strong selectivity, or lowering the criterion to include neurons with weak selectivity, did not affect the results—in all cases the PMC encoded both the response and the rule before the PFC.

We recorded from the PMC after we had recorded from the PFC. This raises the possibility that the faster encoding that we observed in the PMC might have been a result of practice as the monkeys became more experienced at performing the task. To address this issue, we showed that when the PFC and PMC sessions were equated in terms of behavioral performance, the latency differences were still clearly apparent. Nevertheless, it could still be argued that with repeated practice the task becomes more strongly encoded in the brain, although this does

not necessarily correlate with an improvement in behavioral performance. To firmly address this issue will require future experimentation.

In conclusion, by using a paradigm that independently varied the sensory and motor components of a task, we were able to provide evidence that, although there is ample overlap in the neuronal properties of the PFC and PMC, functional dissociations are also evident. This distribution and intermixing of sensory and motor signals can provide an infrastructure for sensorimotor integration in the frontal lobe, although there are relative specializations between areas consistent with their respective positions in a perception–action processing hierarchy.

The authors thank M. Wicherski for valuable comments.

DISCLOSURES

This work was supported by National Institute of Neurological Disorders and Stroke Grant NS-345145. J. D. Wallis was supported by the Wellcome Trust and the McDonnell-Pew Foundation.

REFERENCES

- Asaad WF, Rainer G, and Miller EK. Neural activity in the primate prefrontal cortex during associative learning. *Neuron* 21: 1399–1407, 1998.
- Barbas H and Pandya D. Patterns of connections of the prefrontal cortex in the rhesus monkey associated with cortical architecture. In: *Frontal Lobe Function and Dysfunction*, edited by Levin HS, Eisenberg HM, and Benton AL. New York: Oxford University Press, 1991, p. 35–58.
- Black P, Markowitz, RS, and Cianci, SN. Recovery of motor function after lesions in motor cortex in monkeys. In: *Outcome of Severe Damage to the Central Nervous System, CIBA Symposium*. Amsterdam: Elsevier, 1975, p. 65–70.
- Boussaoud D and Wise SP. Primate frontal cortex: effects of stimulus and movement. *Exp Brain Res* 95: 28–40, 1993a.
- Boussaoud D and Wise SP. Primate frontal cortex: neuronal activity following attentional versus intentional cues. *Exp Brain Res* 95: 15–27, 1993b.
- Brodmann K. *Vergleichende Lokalisationslehre der Grosshirinde in ihren Prinzipien dargestellt auf Grund des Zellenbaues*. Leipzig, Germany: Barth, 1909.
- Bussey TJ, Wise SP, and Murray EA. The role of ventral and orbital prefrontal cortex in conditional visuomotor learning and strategy use in rhesus monkeys (*Macaca mulatta*). *Behav Neurosci* 115: 971–982, 2001.
- Carmichael ST and Price JL. Sensory and premotor connections of the orbital and medial prefrontal cortex of macaque monkeys. *J Comp Neurol* 363: 642–664, 1995.
- Chen LL and Wise SP. Neuronal activity in the supplementary eye field during acquisition of conditional oculomotor associations. *J Neurophysiol* 73: 1101–1121, 1995a.
- Chen LL and Wise SP. Supplementary eye field contrasted with the frontal eye field during acquisition of conditional oculomotor associations. *J Neurophysiol* 73: 1122–1134, 1995b.
- Chen LL and Wise SP. Evolution of directional preferences in the supplementary eye field during acquisition of conditional oculomotor associations. *J Neurosci* 16: 3067–3081, 1996.
- Cohen J. *Statistical Power Analysis for the Behavioral Sciences*. New York: Academic Press, 1988.
- Constantinidis C, Franowicz MN, and Goldman-Rakic PS. The sensory nature of mnemonic representation in the primate prefrontal cortex. *Nat Neurosci* 4: 311–316, 2001.
- Dias R, Robbins TW, and Roberts AC. Dissociation in prefrontal cortex of affective and attentional shifts. *Nature* 380: 69–72, 1996.
- Dias R, Robbins TW, and Roberts AC. Dissociable forms of inhibitory control within prefrontal cortex with an analog of the Wisconsin Card Sort Test: restriction to novel situations and independence from “on-line” processing. *J Neurosci* 17: 9285–9297, 1997.
- di Pellegrino G and Wise SP. A neurophysiological comparison of three distinct regions of the primate frontal lobe. *Brain* 114: 951–978, 1991.
- di Pellegrino G and Wise SP. Visuospatial versus visuomotor activity in the premotor and prefrontal cortex of a primate. *J Neurosci* 13: 1227–1243, 1993.
- Duncan J. An adaptive coding model of neural function in prefrontal cortex. *Nat Rev Neurosci* 2: 820–829, 2001.
- Funahashi S, Bruce CJ, and Goldman-Rakic PS. Mnemonic coding of visual space in the monkey’s dorsolateral prefrontal cortex. *J Neurophysiol* 61: 331–349, 1989.
- Fuster JM. *The Prefrontal Cortex: Anatomy, Physiology and Neuropsychology of the Frontal Lobe*. Baltimore, MD: Lippincott/Williams & Wilkins, 1997.
- Fuster JM, Bauer RH, and Jervey JP. Cellular discharge in the dorsolateral prefrontal cortex of the monkey in cognitive tasks. *Exp Neurol* 77: 679–694, 1982.
- Giguere M and Goldman-Rakic PS. Mediodorsal nucleus: areal, laminar, and tangential distribution of afferents and efferents in the frontal lobe of rhesus monkeys. *J Comp Neurol* 277: 195–213, 1988.
- Godschalk M, Lemon RN, Kuypers HG, and van der Steen J. The involvement of monkey premotor cortex neurones in preparation of visually cued arm movements. *Behav Brain Res* 18: 143–157, 1985.
- Gross CG. How inferior temporal cortex became a visual area. *Cereb Cortex* 4: 455–469, 1994.
- Grueninger WE and Pribram KH. Effects of spatial and nonspatial distractors on performance latency of monkeys with frontal lesions. *J Comp Physiol Psychol* 68: 203–209, 1969.
- Halsband U and Passingham RE. Premotor cortex and the conditions for movement in monkeys (*Macaca fascicularis*). *Behav Brain Res* 18: 269–277, 1985.
- Hernandez A, Zainos A, and Romo R. Temporal evolution of a decision-making process in medial premotor cortex. *Neuron* 33: 959–972, 2002.
- Kalaska JF and Crammond DJ. Deciding not to GO: neuronal correlates of response selection in a GO/NOGO task in primate premotor and parietal cortex. *Cereb Cortex* 5: 410–428, 1995.
- Knight RT. Decreased response to novel stimuli after prefrontal lesions in man. *Electroencephalogr Clin Neurophysiol* 59: 9–20, 1984.
- Kubota K and Funahashi S. Direction-specific activities of dorsolateral prefrontal and motor cortex pyramidal tract neurons during visual tracking. *J Neurophysiol* 47: 362–376, 1982.
- Matelli M, Luppino G, and Rizzolatti G. Patterns of cytochrome oxidase activity in the frontal agranular cortex of the macaque monkey. *Behav Brain Res* 18: 125–136, 1985.
- Miller EK and Cohen JD. An integrative theory of prefrontal cortex function. *Annu Rev Neurosci* 24: 167–202, 2001.
- Miller EK, Erickson CA, and Desimone R. Neural mechanisms of visual working memory in prefrontal cortex of the macaque. *J Neurosci* 16: 5154–5167, 1996.
- Miller EK, Li L, and Desimone R. Activity of neurons in anterior inferior temporal cortex during a short-term memory task. *J Neurosci* 13: 1460–1478, 1993.
- Milner B. Effects of different brain lesions on card sorting. *Arch Neurol* 9: 100–110, 1963.
- Mitz AR, Godschalk M, and Wise SP. Learning-dependent neuronal activity in the premotor cortex: activity during the acquisition of conditional motor associations. *J Neurosci* 11: 1855–1872, 1991.
- Monchi O, Petrides M, Petre V, Worsley K, and Dagher A. Wisconsin Card Sorting revisited: distinct neural circuits participating in different stages of the task identified by event-related functional magnetic resonance imaging. *J Neurosci* 21: 7733–7741, 2001.
- Murray EA, Bussey TJ, and Wise SP. Role of prefrontal cortex in a network for arbitrary visuomotor mapping. *Exp Brain Res* 133: 114–129, 2000.
- Nelson HE. A modified card sorting test sensitive to frontal lobe defects. *Cortex* 12: 313–324, 1976.
- Niki H. Differential activity of prefrontal units during right and left delayed response trials. *Brain Res* 70: 346–349, 1974a.
- Niki H. Prefrontal unit activity during delayed alternation in the monkey. I. Relation to direction of response. *Brain Res* 68: 185–196, 1974b.
- Niki H. Prefrontal unit activity during delayed alternation in the monkey. II. Relation to absolute versus relative direction of response. *Brain Res* 68: 197–204, 1974c.
- Owen AM, Roberts AC, Polkey CE, Sahakian BJ, and Robbins TW. Extra-dimensional versus intra-dimensional set shifting performance following frontal lobe excisions, temporal lobe excisions or amygdalo-hippocampectomy in man. *Neuropsychologia* 29: 993–1006, 1991.
- Pandya DN and Barnes CL. Architecture and connections of the frontal lobe. In: *The Frontal Lobes Revisited*, edited by Perecman E. New York: The IRBN Press, 1987, p. 41–72.

- Pandya DN and Yeterian EH.** Prefrontal cortex in relation to other cortical areas in rhesus monkey: architecture and connections. *Prog Brain Res* 85: 63–94, 1990.
- Parker A and Gaffan D.** Memory after frontal/temporal disconnection in monkeys: conditional and non-conditional tasks, unilateral and bilateral frontal lesions. *Neuropsychologia* 36: 259–271, 1998.
- Passingham RE.** *The Frontal Lobes and Voluntary Action.* Oxford, UK: Oxford University Press, 1993.
- Passingham RE, Perry VH, and Wilkinson F.** The long-term effects of removal of sensorimotor cortex in infant and adult rhesus monkeys. *Brain* 106: 675–705, 1983.
- Petrides M.** Motor conditional associative-learning after selective prefrontal lesions in the monkey. *Behav Brain Res* 5: 407–413, 1982.
- Petrides M.** Deficits in non-spatial conditional associative learning after periarculate lesions in the monkey. *Behav Brain Res* 16: 95–101, 1985.
- Petrides M and Pandya DN.** Comparative architectonic analysis of the human and macaque frontal cortex. In: *Handbook of Neuropsychology*, edited by Boller F and Grafman J. New York: Elsevier, 1994, p. 17–57.
- Podbros LZ, Stamm JS, and Denaro FJ.** Associative function of the arcuate segment of the monkey's prefrontal cortex. *Physiol Behav* 24: 103–109, 1980.
- Ragozzino ME, Wilcox C, Raso M, and Kesner RP.** Involvement of rodent prefrontal cortex subregions in strategy switching. *Behav Neurosci* 113: 32–41, 1999.
- Raichle ME, Fiez JA, Videen TO, MacLeod AM, Pardo JV, Fox PT, and Petersen SE.** Practice-related changes in human brain functional anatomy during nonmotor learning. *Cereb Cortex* 4: 8–26, 1994.
- Ramus SJ and Eichenbaum H.** Neural correlates of olfactory recognition memory in the rat orbitofrontal cortex. *J Neurosci* 20: 8199–8208, 2000.
- Roberts AC and Wallis JD.** Inhibitory control and affective processing in the prefrontal cortex: neuropsychological studies in the common marmoset. *Cereb Cortex* 10: 252–262, 2000.
- Sakagami M and Niki H.** Encoding of behavioral significance of visual stimuli by primate prefrontal neurons: relation to relevant task conditions. *Exp Brain Res* 97: 423–436, 1994a.
- Sakagami M and Niki H.** Spatial selectivity of go/no-go neurons in monkey prefrontal cortex. *Exp Brain Res* 100: 165–169, 1994b.
- Shallice T.** Specific impairments of planning. *Philos Trans R Soc Lond B Biol Sci* 298: 199–209, 1982.
- Shallice T and Evans ME.** The involvement of the frontal lobes in cognitive estimation. *Cortex* 14: 294–303, 1978.
- Siwek DF and Pandya DN.** Prefrontal projections to the mediodorsal nucleus of the thalamus in the rhesus monkey. *J Comp Neurol* 312: 509–524, 1991.
- Stamm JS.** Functional dissociation between the inferior and arcuate segments of dorsolateral prefrontal cortex in the monkey. *Neuropsychologia* 11: 181–190, 1973.
- Stepien I.** The magnet reaction, a symptom of prefrontal ablation. *Acta Neurobiol Exp* 34: 145–160, 1974.
- Stuss DT, Levine B, Alexander MP, Hong J, Palumbo C, Hamer L, Murphy KJ, and Izukawa D.** Wisconsin Card Sorting Test performance in patients with focal frontal and posterior brain damage: effects of lesion location and test structure on separable cognitive processes. *Neuropsychologia* 38: 388–402, 2000.
- Walker E.** A cytoarchitectural study of the prefrontal area of the macaque monkey. *J Comp Neurol* 98: 59–96, 1940.
- Wallis JD, Anderson KC, and Miller EK.** Single neurons in prefrontal cortex encode abstract rules. *Nature* 411: 953–956, 2001a.
- Wallis JD, Dias R, Robbins TW, and Roberts AC.** Dissociable contributions of the orbitofrontal and lateral prefrontal cortex of the marmoset to performance on a detour reaching task. *Eur J Neurosci* 13: 1797–1808, 2001b.
- Watanabe M.** Prefrontal unit activity during delayed conditional Go/No-Go discrimination in the monkey. I. Relation to the stimulus. *Brain Res* 382: 1–14, 1986a.
- Watanabe M.** Prefrontal unit activity during delayed conditional Go/No-Go discrimination in the monkey. II. Relation to Go and No-Go responses. *Brain Res* 382: 15–27, 1986b.
- Weinrich M and Wise SP.** The premotor cortex of the monkey. *J Neurosci* 2: 1329–1345, 1982.
- Weinrich M, Wise SP, and Mauritz KH.** A neurophysiological study of the premotor cortex in the rhesus monkey. *Brain* 107: 385–414, 1984.
- Wise SP and Mauritz KH.** Set-related neuronal activity in the premotor cortex of rhesus monkeys: effects of changes in motor set. *Proc R Soc Lond B Biol Sci* 223: 331–354, 1985.
- Wise SP, Murray EA, and Gerfen CR.** The frontal cortex-basal ganglia system in primates. *Crit Rev Neurobiol* 10: 317–356, 1996.